Axial Vibration Study of a Mobile Fan Motor

Chien-Chang Wang[1], Yeong-Der Yao[1,2], Kun-Yi Liang[3], Chung-Chun Huang[3], Yu-Choung Chang[3], and David A. Lowther[4]

[1]Department of Materials Science and Engineering, National Chiao Tung University, Hsinchu, 300 Taiwan
[2]Graduate Institute of Applied Science and Engineering, Fu Jen Catholic University, Taipei 242, Taiwan
[3]Energy and Environment Research Laboratories, Industrial Technology Research Institute, Hsinchu 310, Taiwan
[4]Department of Electrical & Computer Engineering, McGill University, Montreal, Quebec H3A2A7, Canada

A method observing both radial and axial vibrations of time domain and frequency spectrum was studied to investigate the axial load effect of a flat-type brushless dc fan motor operating with and without the rated axial thrust force. When the developed small motor does not exhibit an intrinsically excited unbalanced magnetic force (UMF), the axial force leads to a minor contribution to the growth of the axial vibration. However, when the UMF is intrinsically excited, the preload can enormously decrease the undesired axial vibration. The ratio of the axial vibration of the prototype with the asymmetric magnetic sheet to the one without the sheet is experimentally observed around 55 percent. It demonstrates that axial load plays an effective and crucial factor in controlling the axial vibration of the mobile fan motor.

***Index Terms*—Axial load, motor, preload, vibration.**

I. Introduction

A MOBILE FAN motor for use in portable devices such as cell phones, ultra-mobile PCs, and mobile internet devices must be designed with low power consumption, low noise, and low vibration. Since the small fan is used for cooling the main digital signal processor chips or other integrated circuits, large vibration of the fan may become confused with an intentional vibration indicating a paging signal. So, ideally, the vibration should be reduced as much as possible. Therefore, the issue of suppressing the vibration of a mobile fan motor is very important.

From the view of bearing design, in this case a sleeve bearing, the axial load functions as an attractive force to prevent the rotor from jumping out of the micro motor when it encounters an external shock in the static or dynamic status. In general, for a flat-type motor, the axial preload is introduced using the magnetic attraction force between a permanent magnet (PM) and a magnetic sheet. Unfortunately, along with the axial thrust force, an Unbalanced Magnetic Force (UMF) is simultaneously created; i.e., they can not be decoupled for this type of motor. As is known, UMF and cogging torque are main factors contributing to magnetically induced vibration. Jang *et al.* [1] performed an experimental study to show that rotor and stator eccentricities mainly generate a radial vibration at the first harmonic frequency and at the harmonics of the pole number. Hartman *et al.* [2] reported that the sources of UMF fall into the following categories: an eccentric rotor, an eccentric stator, and uneven magnetization. Yao *et al.* [3], [4] showed that the mechanism of the reduction of cogging is illustrated by the minimum net integral of the product of normal and tangential magnetic flux with respect to the contour between the stator and rotor; and they proposed a method achieving a high efficiency and low cogging torque motor by altering the magnetization profiles of the permanent magnet and the design of the teeth of the stator in a motor. A few researchers [5], [6] have focused on the characteristics of UMF related to a motor, adopting numerical and analytical approaches. However, the axial load effect, which accompanies UMF and results in the vibration of a miniature motor, is not addressed. The main goal of this paper is to understand the axial load effect related to the axial vibration in the development of a mobile fan motor.

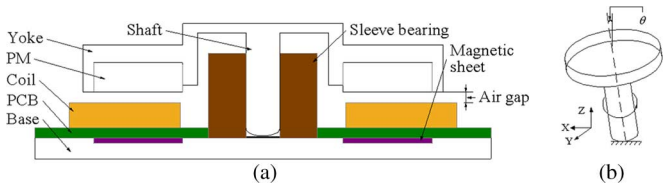

Fig. 1. Sketch of (a) the micro motor and (b) the tilted rotor.

The axial vibration of the micro motor is due to three essential factors: the radial vibration, the UMF, and the axial load. These are studied and analyzed. First, this paper deals with a simple physical model of the sleeve bearing motor to determine the relation between radial and axial vibrations, and it is presumed that the magnitude in the 1X (where X designates the fundamental frequency) axial vibration harmonic should be a fraction of the radial one because the axial one is only a sine of a tilt angle times the magnitude of the 1X radial vibration harmonic due to the mass unbalance of the rotor. This assumption is experimentally validated. In addition, the frequency contents of the axial load coupled with the UMF for micro motors are numerically analyzed using FEM and compared with the experimental results. Furthermore, both the axial load effect with and without excited UMF are reported.

II. Design and Force Calculation

Fig. 1(a) shows the sketch of the developed motor. It consists of a spindle motor, a sleeve bearing system, a PCB, and a Base.

Manuscript received October 27, 2009; accepted January 22, 2010. Current version published May 19, 2010. Corresponding authors: Y. D. Yao and C. C. Wang (e-mail: ydyao@phys.sinica.edu.tw; JamesCCW@itri.org.tw).

Color versions of one or more of the figures in this paper are available online at http://ieeexplore.ieee.org.

Digital Object Identifier 10.1109/TMAG.2010.2042143

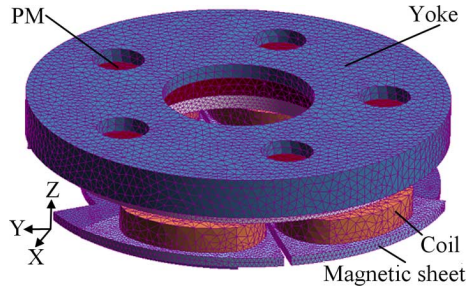

Fig. 2. FEM model of the mobile fan motor.

The motor has 6 slots and 8 poles. The axial air gap between the coil and PM is 3×10^{-4} m; the PM is made of high energy product NdFeB with an inner radius of 2×10^{-3} m, an axial length of 5×10^{-3} m, and an outer radius of 4×10^{-3} m. Outside the PM, an iron yoke with a radial thickness of 6×10^{-4} m is mounted. The rotational speed of the micro motor is 6360 rpm, and the rated current is below 25 mA. The sleeve bearing has an inner radius of 4×10^{-4} m, an outer radius of 8×10^{-4} m, and an axial length of 2.5×10^{-3} m, and the clearance is 4 micro meters. To identify the model mentioned above, identical motors, M1 to M3, are the type with a symmetric magnetic sheet to preload the rotor; also, motor M1 is utilized to study the axial load effect without UMF (motor M1P). To investigate the axial load effect under UMF, the second type micro motor, M4, with an asymmetric magnetic sheet, has been fabricated; the ratio of pole number to slot number is 6:2, and the other mechanical constraints are the same as those of the first type. In general, the shape of the magnetic sheet in motor M4 should be asymmetric in order to avoid the dead point [7]. M1P and M4P designate motors M1 and M4 without the sheet, respectively.

Fig. 1(b) displays the simplified model of a rotating rotor of the small motor. Referring to Newton's second law, the unbalance force of the rotor can be represented as

$$F = \overline{m}\,\overline{e}\,\omega^2 \sin(\theta) \tag{1}$$

where $\overline{m}$, $\overline{e}$, and ω denote the mass unbalance of the rotor, the rotor eccentricity, and rotor rotational speed, respectively. Since the bearing clearance is only 4 μm, it is believed that the tilt angle theta rotates about the Y-axis, as shown in Fig. 1(b), and can be small enough to lead to the result that the undesired axial vibration force is only a fraction of the radial one for a well designed sleeve bearing motor. Therefore, once the axial vibration of a motor is greater than the radial one, then both the preload and UMF may be regarded as the principal contributors to the vibration. Definitely, based on this assumption, the mass unbalance of each motor has to be maintained close to a level which avoids propagating radial vibration which, in turn, leads to the rise of the axial vibration.

Fig. 2 presents the FEM model of the proposed motor with 892,892 tetrahedral elements. The sampling mechanical angle interval of one degree is utilized in estimating the preload force distribution of the motor. The preload profiles versus mechanical rotation angles and the corresponding frequency spectra after the FEM calculation are shown in Fig. 3. The mean values of the axial forces for motors M1, M4, and M4P are 32.11, 27.95, and 3.07 mN, respectively. While the axial force curve for motor M1 contains only a DC term, those of motors M4 and M4P contain 6X and 12X axial force harmonics, and the first two peak values in magnitude for motors M4 and M4P both occur at 6X (M4: 1.66 mN; M4P: 1.10 mN) and 12X (M4: 0.12 mN; M4P: 0.10mN) harmonics. Nonetheless, the 1X component is not generated; i.e., although the UMFs are induced in the motors M4 and M4P, they do not contribute to the 1X harmonic. For motors M4 and M4P, mass unbalance of these two motors are almost the same, and the simulated result indicates that the UMFs of these two motors do not contain the 1X axial force harmonic (which dominates the axial vibration of time domain). These results suggest that the axial load will effectively affect the axial vibration of the motors.

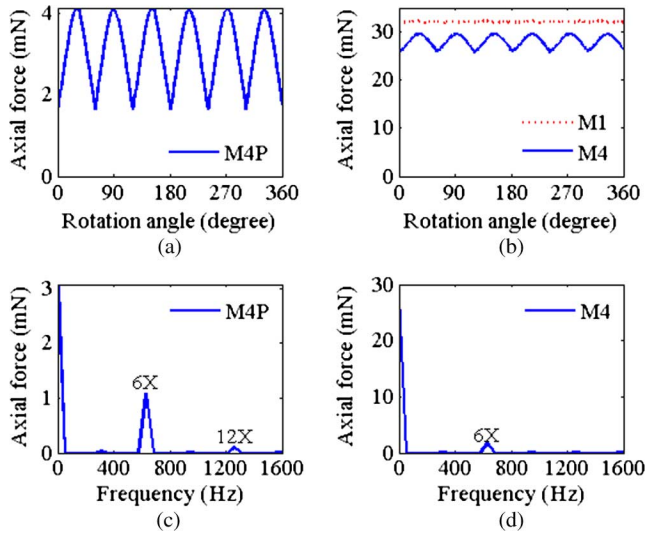

Fig. 3. Simulated axial loads of spatial domain for motors: (a) M4P; and (b) M1 and M4; the frequency spectra for motors: (c) M4P; and (d) M4.

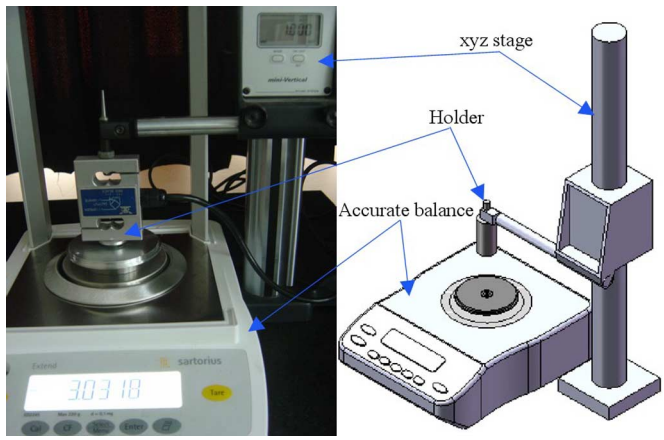

Fig. 4. Structure of the test setup for the axial load measurement.

III. Experimental Measurements

For measurement of the axial load, the rotor was tightly fixed to an accurate balance (see Fig. 4), and the magnetic sheet was arranged above and locked at a manual xyz stage. After a centering device was applied to center the rotor and the magnetic sheet, the axial attraction force versus different axial

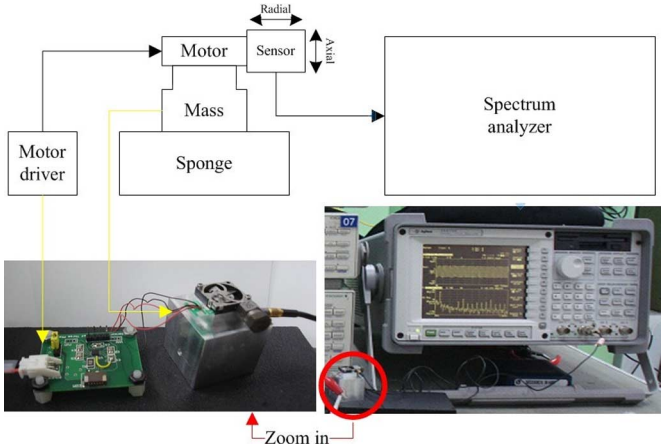

Fig. 5. Configuration of the test setup for vibration measurement.

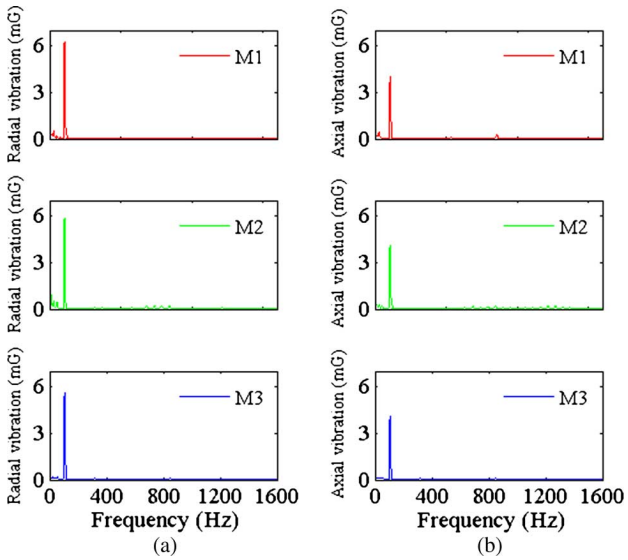

Fig. 6. Frequency spectra of (a) radial and (b) axial vibrations for motors M1 to M3.

air gaps was obtained. As the working distance was reached, the axial forces for M1 and M4 were 32.48 mN and 26.83 mN, respectively, which is consistent with the numerical results. To verify the vibration properties of the mobile fan motor, the measurement plant was constructed as shown in Fig. 5. A precise accelerometer was utilized to detect the vibration. While the testing was performed, the motor was rotating at the rated speed of 6360 rpm. The accelerometer was attached to the motor to sense the traveling vibration signals; then the vibration was calculated and recorded by a spectrum analyzer. Finally, the vibration harmonics can be determined by using the fast Fourier transform method.

Three motors, M1 to M3, were prepared for identifying the simple model mentioned above. The corresponding frequency spectra of radial and axial vibrations are shown in Fig. 6. It is clear that the magnitudes of the 1X components are the dominant reasons for the vibrations of the motors in both the radial and axial directions. Table I summarizes the magnitudes of the 1X harmonics of the radial and axial vibrations for these motors; the ratio of the axial vibration to the radial one is between

TABLE I
MAGNITUDES OF 1X RADIAL AND AXIAL VIBRATION HARMONICS FOR MOTORS M1P AND M1 TO M3

Motor No.	Radial (mG)	Axial (mG)
M1P	6.279	3.051
M1	6.255	4.041
M2	5.850	4.124
M3	5.624	4.134

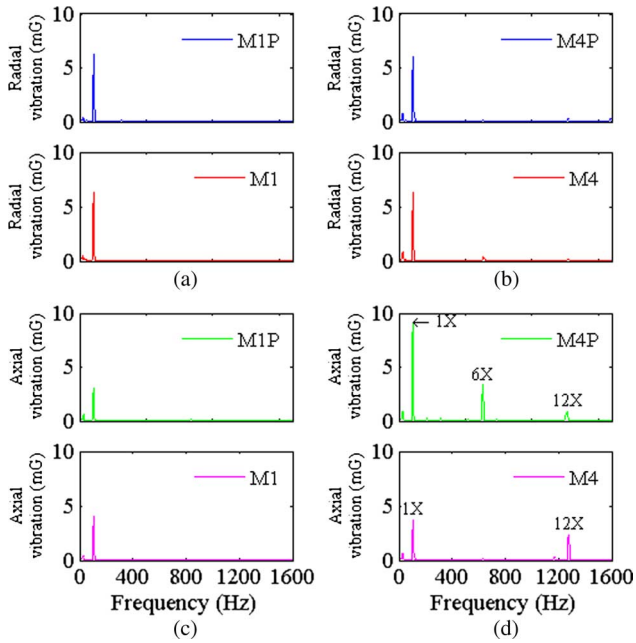

Fig. 7. Frequency spectra of the radial and axial vibrations for motors. Radial vibration: (a) M1P and M1; and (b) M4P and M4; axial vibration: (c) M1P and M1; and (d) M4P and M4.

65 and 75 percent, which supports the model that the axial vibration of the small motor is only a fraction of the radial one. In addition, the result reveals that mass unbalance of the rotor is a key factor affecting the vibration of the motors.

IV. RESULTS AND DISCUSSION

Fig. 7 shows shows frequency spectra of radial and axial vibrations for the motors M1P (motor M1 without the magnetic sheet), M1, M4P (motor M4 without the magnetic sheet), and M4. It indicates that the 1X harmonic of the axial vibration is slightly increased to a value of 0.99 mG (see Table I, where $1\mathrm{G} = 9.8\,\mathrm{m/s^2}$) after the symmetric magnetic sheet is installed; i.e., the preload has slightly increased the axial vibration and its 1X harmonic. Figs. 8(a) and 8(b) show the axial vibration of the motors M1P and M1, respectively, and the amplitudes in peak-to-peak (pk-pk) are 11 mG and 15 mG for the former and latter, respectively.

Comparing the two graphs in Fig. 7(d), the motor M4P (top graph) demonstrates the 6X and 12X axial vibration harmonics due to the UMF, while the motor M4 merely includes the latter harmonic (see Table II). However, these two harmonics (6X and 12X) in magnitude were predicted by FEM analysis. The unexpected disappearance of the 6X harmonic for the motor M4 is believed to be associated with its asymmetrical coil (this means

TABLE II
MAGNITUDES OF RADIAL AND AXIAL VIBRATION HARMONICS FOR MOTORS M4P AND M4

Frequency	1X		6X		12X	
Motor No.	Radial	Axial	Radial	Axial	Radial	Axial
M4P	5.986	9.083	0.163	3.382	0.168	0.879
M4	6.266	3.680	0.403	0.074	0.236	2.352

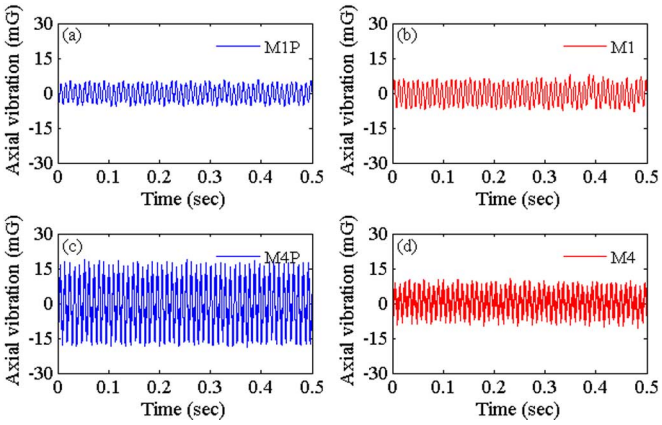

Fig. 8. Axial vibrations for motors: (a) M1P; (b) M1; (c) M4P; and (d) M4.

some defects in the coil were developed during the fabrication process), and the induced UMF harmonics due to the defects are related to the pole number of magnets [2].

As mentioned earlier, the axial vibration results from three primary contributors: the UMF, the radial vibration, and the axial load. According to the numerical results, the UMFs of these two motors do not contribute to the 1X axial vibration harmonic. In addition, the measured magnitudes of the 1X radial vibration harmonic for these two motors are maintained nearly the same (M4P:5.986 mG; and 6.266 mG). However, the measured magnitude of the 1X axial vibration harmonic is enormously raised, and the ratio of this harmonic of motor M4 to motor M4P is approximately 41 percent. The reason might be that the lack of axial load leads to the growth of the magnitude of the 1X axial vibration harmonic; i.e., a weak axial load may result in an increase in the magnitude of the 1X axial vibration harmonic if the shaft is loose. Therefore, the axial preload plays an essential function in the reduction of the 1X axial vibration harmonic of the micro motor. Furthermore, comparing the axial vibrations of motors M4 and M4P reveals that the axial vibration is significantly reduced for motor M4. The amplitudes (pk-pk) of the axial vibrations for the motors M4P and M4 are 38 mG and 21 mG, respectively (see Figs. 8(c) and 8(d)).

V. CONCLUSION

When a symmetric magnetic sheet is utilized to produce the axial force for the developed micro motor with 6 slots/8 poles, the preload slightly increases the axial vibration of the spindle; however, when the asymmetric magnetic sheet is employed to preload the motor with 2 slots/6 poles and the intrinsically excited UMF, the preload significantly decreases the magnitude of the 1X axial vibration harmonic. Moreover, comparing the axial vibration of the small motor without and with the asymmetric magnetic sheet, the magnitudes of the axial vibration and its 1X harmonic for the latter are 45 and 59 percent reduction of the former, respectively. It appears that the axial load highly affects the axial vibration of the mobile motor with an UMF.

ACKNOWLEDGMENT

This work was supported by the National Science Council of Taiwan under Grant NSC98-2112-M-030-002, by the Sapintia Education Foundation, and by Research Grant 2010 from Fu Jen University.

REFERENCES

[1] C. I. Lee and G. H. Jang, "Experimental measurement and simulated verification of the unbalanced magnetic force in brushless DC motors," *IEEE Trans. Magn.*, vol. 44, no. 11, pp. 4377–4380, Nov. 2008.
[2] A. Hartman and W. Lorimer, "Undriven vibrations in brushless DC motors," *IEEE Trans. Magn.*, vol. 37, no. 2, pp. 789–792, Mar. 2001.
[3] Y. D. Yao, D. R. Huang, J. C. Wang, S. H. Liou, S. J. Wang, T. F. Ying, and D. Y. Chiang, "Simulation study of the reduction of cogging torque in permanent magnet motors," *IEEE Trans. Magn.*, vol. 33, no. 5, pp. 4095–4097, Sep. 1997.
[4] Y. D. Yao, D. R. Huang, J. C. Wang, S. J. Wang, T. F. Ying, and D. Y. Chiang, "Study of a high efficiency and low cogging torque spindle motor," *IEEE Trans. Magn.*, vol. 34, no. 2, pp. 465–467, Mar. 1998.
[5] S. X. Chen, Q. D. Zhang, Z. J. Liu, and H. Lin, "Design of fluid bearing spindle motors with controlled unbalanced magnetic forces," *IEEE Trans. Magn.*, vol. 33, no. 5, pp. 2638–2640, Sep. 1997.
[6] T. Yoon, "Magnetically induced vibration in a permanent-magnet brushless DC motor with symmetric pole-slot configuration," *IEEE Trans. Magn.*, vol. 41, no. 6, pp. 2173–2179, Jun. 2005.
[7] C. M. Chao, S. J. Wang, C. P. Liao, D. R. Huang, and T. F. Ying, "Torque and cogging torque in sandwich type CD-ROM spindle motor," *IEEE Trans. Magn.*, vol. 34, no. 2, pp. 471–473, Mar. 1998.